

# Supporting Information

## Simple Approach: Heat Treatment to Improve the Electrochemical Performance of Commonly Used Anode Electrodes for Lithium-Ion Batteries

*Ye Jin, Han Yu, Xinhua Liang \**

Department of Chemical and Biochemical Engineering, Missouri University of Science and  
Technology, Rolla, Missouri 65409, United States

\* Corresponding author. E-mail: [liangxin@mst.edu](mailto:liangxin@mst.edu)

The following additional information is listed in this Supporting Information file, including Table S1, density data of the materials in electrodes; Table S2, weight percentages of F element of the electrodes; Table S3, electrochemical impedance spectra fitting results of electrodes; Table S4, binding energies and atomic concentrations of all cycled electrodes; Figure S1, FTIR spectra of PVDF before and after heat treatment and the TGA curve of PVDF; Figure S2, SEM images of pure active material powders or flakes; Figure S3, SEM images of fresh LTO electrodes with and without heat treatment; Figure S4, porosity and liquid electrolyte uptake of the electrodes with and without heat treatment; Figure S5, SEM image and EDS mapping of the cross-section area of the graphite electrodes; Figure S6, XPS survey spectra of all fresh electrodes; Figure S7, Nyquist plots of the electrodes; Figure S8, cycling performance of LTO and  $\text{TiO}_2$  within 1.0- 3.0 V; Figure S9, CV curves of electrodes at different scan rates; Figure S10, XPS survey spectra of the cycled electrodes; Figure S11, SEM images of fresh LTO electrode without heat treatment; Figure S12, SEM image and EDS mapping of pristine LTO electrode after 500 cycles of charge/discharge; Figure S13, SEM images of fresh  $\text{TiO}_2$  electrode with heat treatment; Figure S14, SEM image and EDS mapping of pristine graphite electrode after 500 cycles of charge/discharge; Figure S15, TEM images of pure  $\text{TiO}_2$  nanoparticles.

**Table S1.** Density data of the materials in electrodes.

		Density (g cm <sup>-3</sup> )
Binder	PVDF	1.76
Conductive material	Carbon black	1.70
	TiO <sub>2</sub>	3.78
Active materials	LTO	3.50
	Graphite	2.21

**Table S2.** Weight percentages of F element of the electrodes obtained from EDS spectra and XPS analysis.

Electrodes		F element (wt. %)	
		EDS spectrum	XPS analysis
LTO	Pristine	4.4	3.4
	250 °C treated	4.0	1.8
TiO <sub>2</sub>	Pristine	4.8	3.5
	250 °C treated	4.6	3.1
Graphite	Pristine	-	2.5
	250 °C treated	-	2.4

**Table S3.** Electrochemical impedance spectra fitting results of electrodes after 1 C cycling performance test.

Electrodes		After formation				After long-term cycling			
		R <sub>f</sub> (Ω)	R <sub>SEI</sub> (Ω)	R <sub>ct</sub> (Ω)	R <sub>tot</sub> (Ω)	R <sub>f</sub> (Ω)	R <sub>SEI</sub> (Ω)	R <sub>ct</sub> (Ω)	R <sub>tot</sub> (Ω)
LTO	Pristine	8.6	39.6	164.6	212.8	20.1	183.6	492.9	696.6
	250 °C treated	6.0	55.2	101.2	162.4	25.2	103.4	290.1	418.7
TiO <sub>2</sub>	Pristine	11.9	10.4	73.6	95.8	19.2	45.3	41.2	105.7
	250 °C treated	9.3	22.1	44.6	75.9	17.6	37.5	34.2	89.2
Graphite	Pristine	15.1	18.0	56.0	89.1	28.8	23.1	76.9	128.8
	250 °C treated	19.8	27.2	38.0	85.0	29.6	30.1	55.4	115.2

**Table S4.** Binding energies (BE) and atomic concentrations (at.%) of three anode materials with and without 250 °C treatment, identified by XPS at the surface of the electrodes.

Anode Material	Orbital	Pristine		250 °C treated		Assignment
		BE (eV)	at %	BE (eV)	at %	
LTO	F 1s	684.4	42.8	684.3	56.0	LiF
		686.8	45.5	686.6	44.0	LiPF <sub>y</sub> O <sub>z</sub>
		687.8	11.7			PVDF
	C 1s	284.8	32.7	284.7	47.4	C-C
		286.4	7.4	286.4	13.3	CH <sub>2</sub>
				288.6	4.3	Li <sub>2</sub> CO <sub>3</sub>
	O 1s	289.9	60.0	289.7	35.1	CF <sub>2</sub>
		528.0	3.5	527.9	2.8	Ti-O from LTO
		529.6	3.5	529.9	8.1	ROLi
		531.5	93.0	531.4	89.1	C=O
TiO <sub>2</sub>	F 1s	684.1	58.3	684.2	100.0	LiF
		686.7	19.2			LiPF <sub>y</sub> O <sub>z</sub>
		688.1	22.5			PVDF
	C 1s	282.7	6.6	282.7	1.2	Ti-C
		284.9	45.0	284.7	55.6	C-C
		286.4	18.5	286.2	18.6	CH <sub>2</sub>
	O 1s			288.7	12.4	Li <sub>2</sub> CO <sub>3</sub>
		290.1	30.0	290.3	12.1	CF <sub>2</sub>
		528.6	33.7	528.3	17.1	Ti-O from TiO <sub>2</sub>
		530.5	8.8			ROLi
		532.0	57.5	531.4	82.9	C=O
Graphite	F 1s	683.7	33.4	684.1	59.2	LiF
		686.1	52.4	686.4	40.8	LiPF <sub>y</sub> O <sub>z</sub>
		687.0	14.2			PVDF
	C 1s	284.8	44.9	284.8	35.8	C-C
		286.4	21.4	286.4	16.5	CH <sub>2</sub>
				288.4	7.7	Li <sub>2</sub> CO <sub>3</sub>
	O 1s	289.7	33.6	289.8	40.0	CF <sub>2</sub>
				527.8	19.8	Li-O
		529.7	15.7	529.3	3.1	ROLi
		530.9	84.3	531.0	77.1	C=O

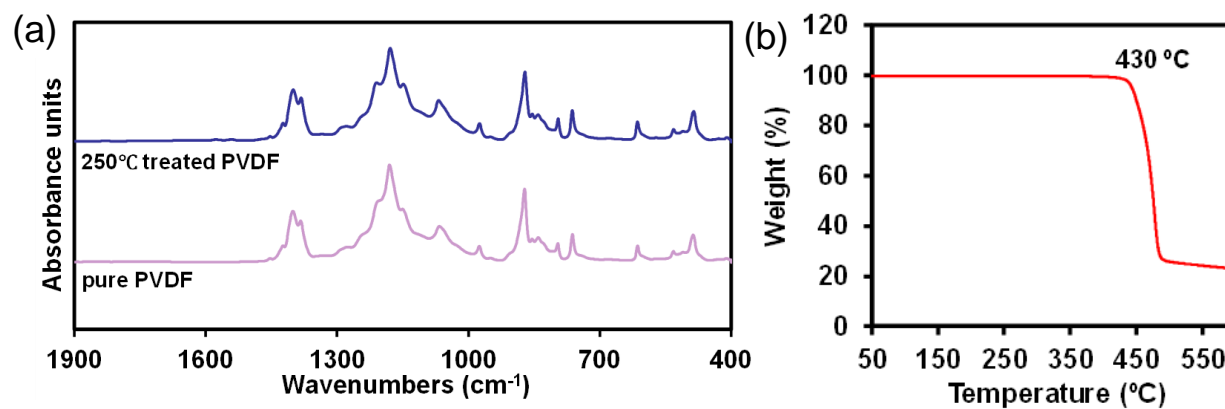


**Figure S1.** (a) FTIR spectra of PVDF before and after 250  $^{\circ}\text{C}$  treatment, and (b) TGA curve of the PVDF used in this study.

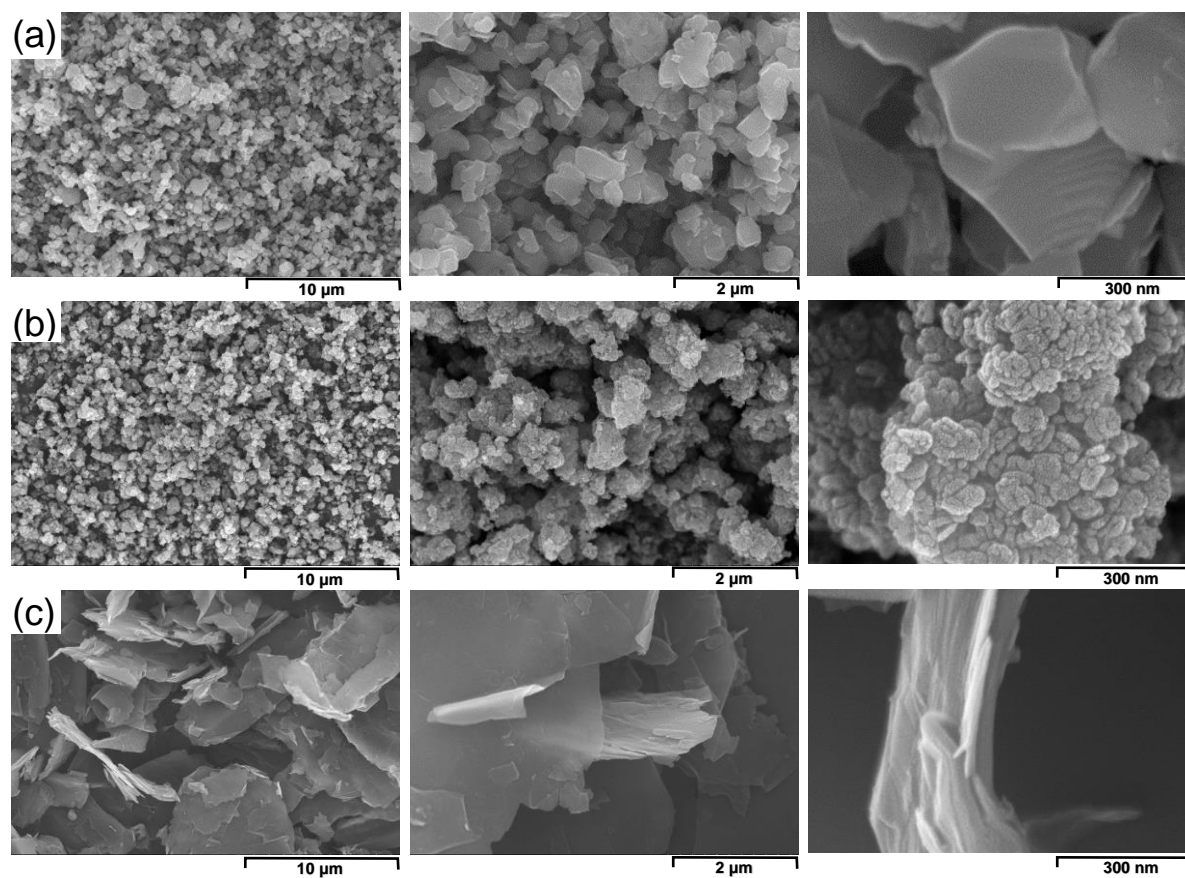


**Figure S2.** SEM images of (a) LTO powders, (b)  $\text{TiO}_2$  powders, and (c) graphite flakes.

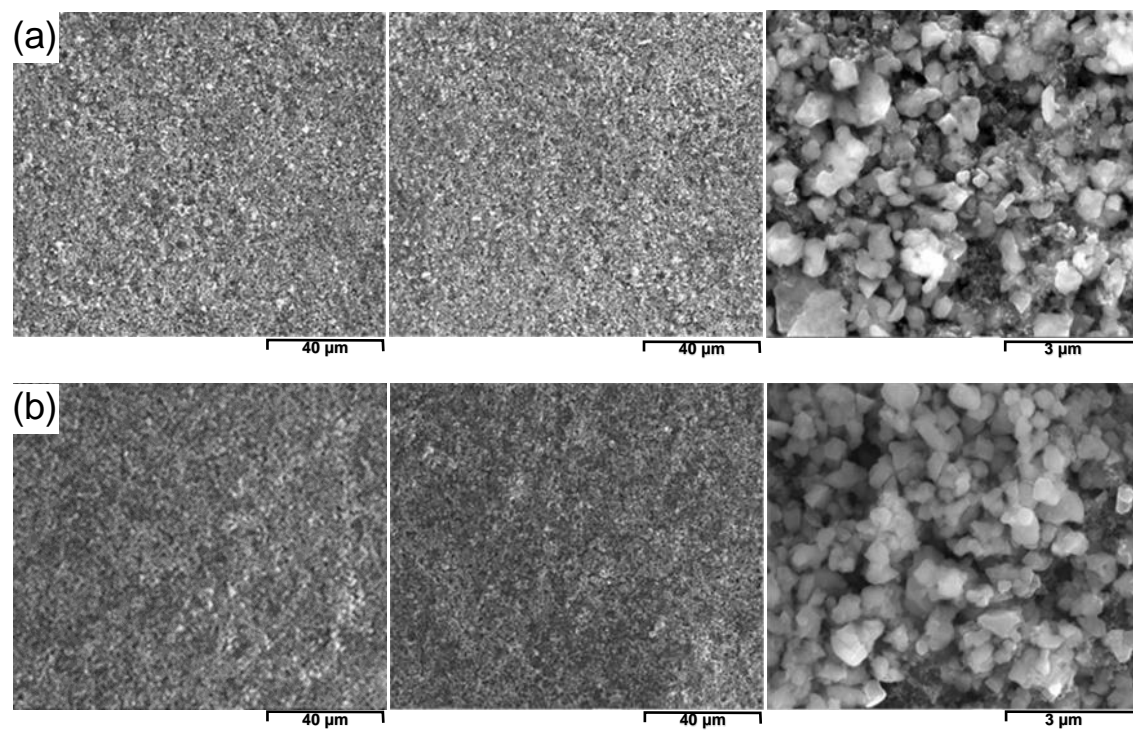


**Figure S3.** SEM images of fresh LTO electrodes (a) before and (b) after 250 °C heat treatment.

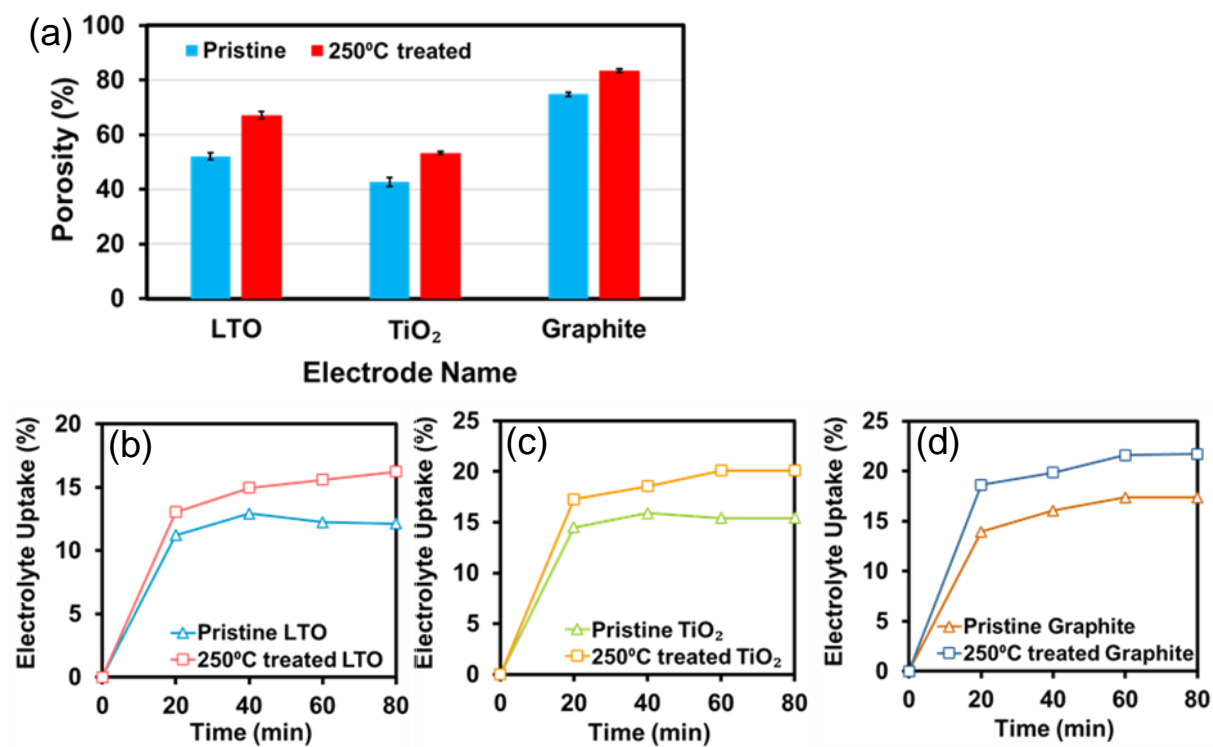


**Figure S4.** (a) Porosity of LTO, TiO<sub>2</sub>, and graphite electrodes before and after 250 °C treatment. Liquid electrolyte weight uptake vs. time for pristine and 250 °C treated electrodes: (b) LTO, (c) TiO<sub>2</sub>, and (d) graphite.

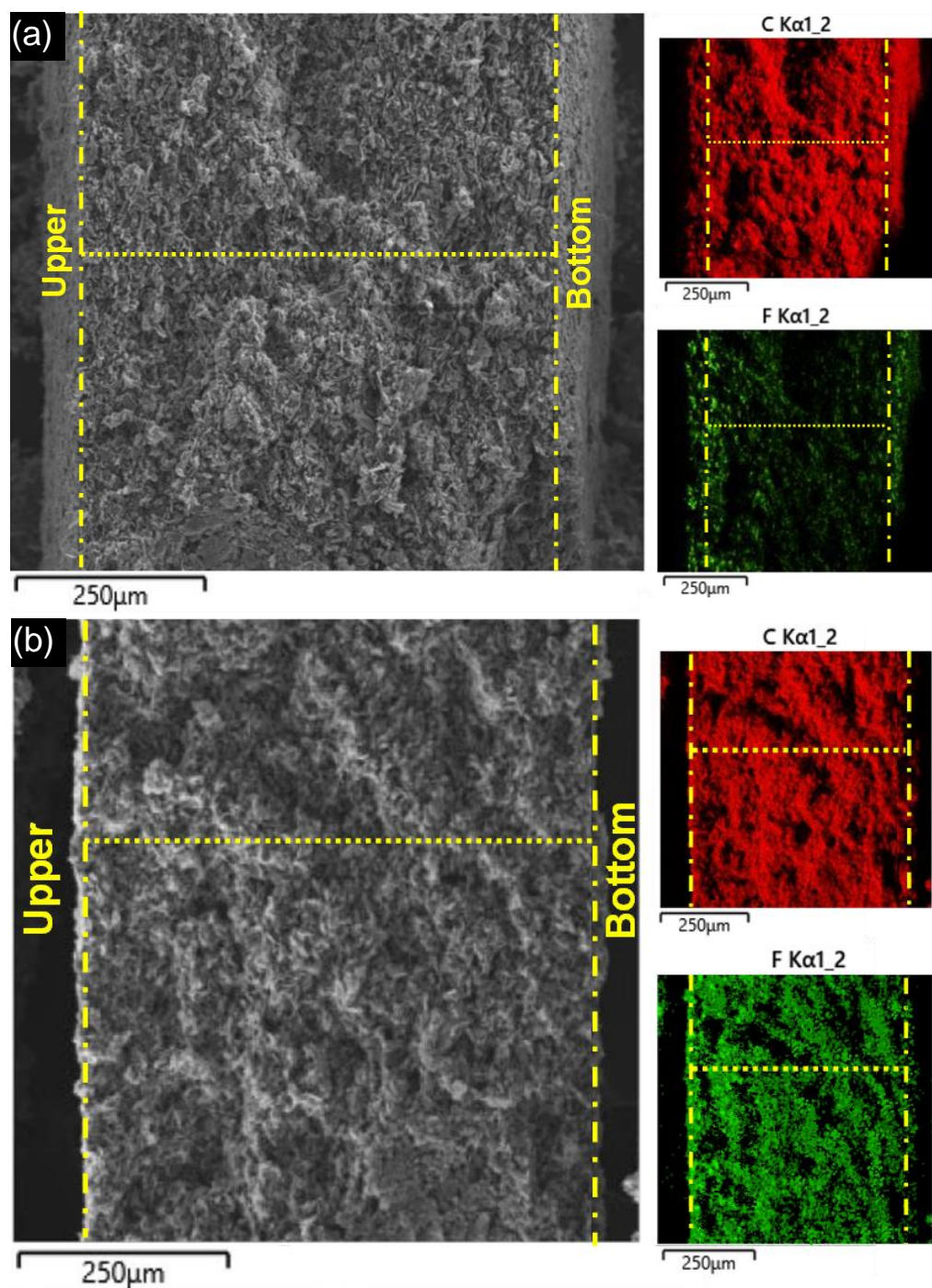


**Figure S5.** SEM images and EDS mapping of the cross-sectional area of (a) pristine graphite electrode and (b) 250 °C treated graphite electrode.



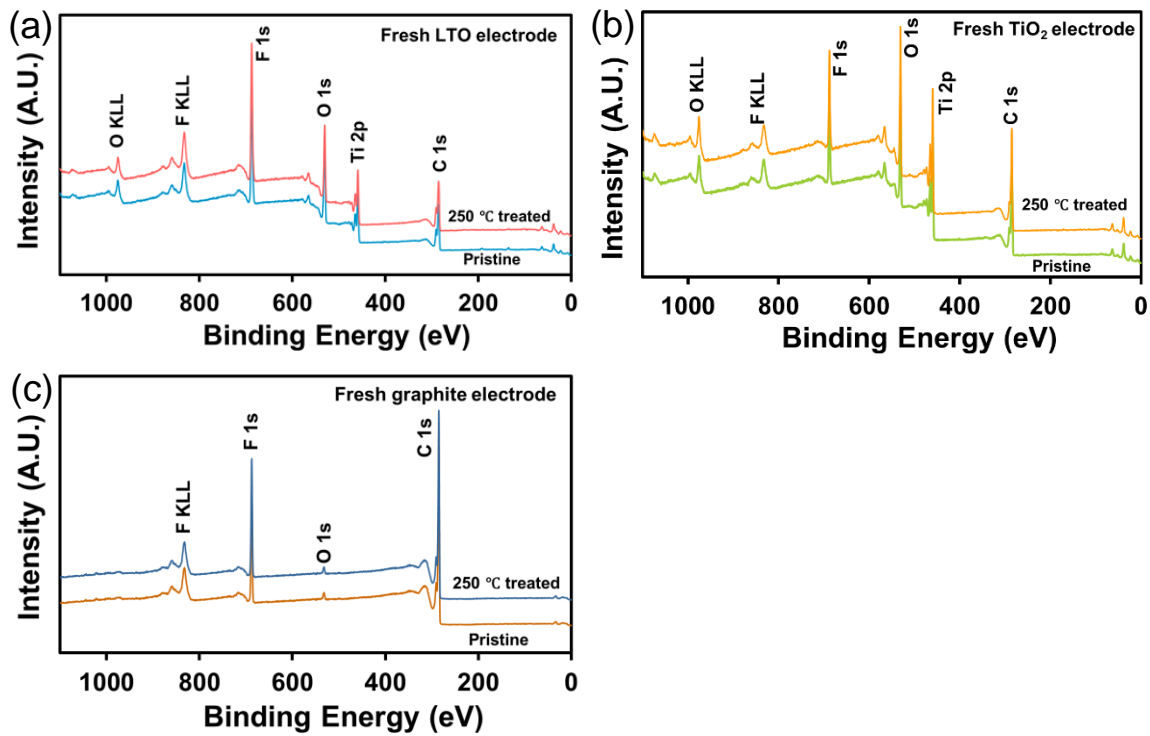


**Figure S6.** XPS survey spectra of fresh electrodes: (a) LTO, (b)  $\text{TiO}_2$ , and (c) graphite.

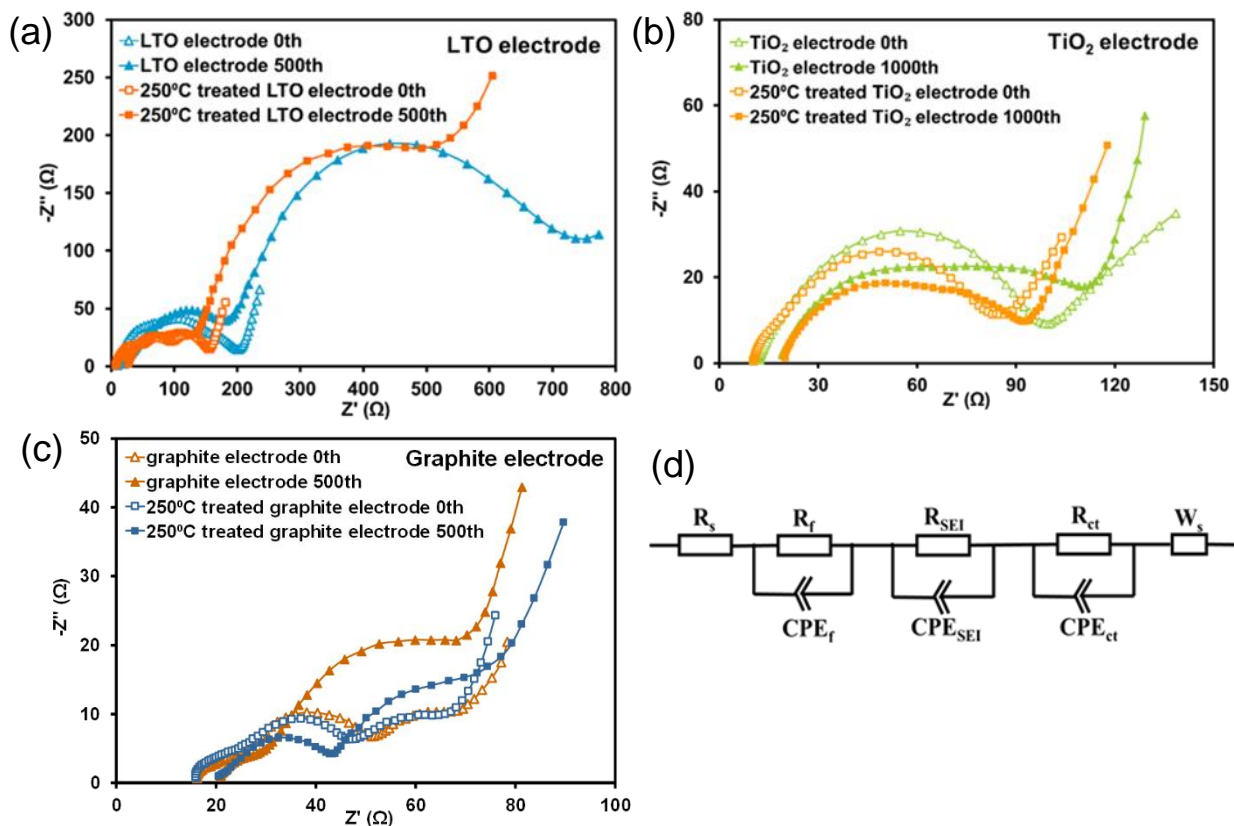


**Figure S7.** Nyquist plots of (a) LTO, (b)  $\text{TiO}_2$ , and (c) graphite electrodes tested at a 1 C rate with a potential range of 0.1 V – 3.0 V at 0<sup>th</sup> (after the formation at a 0.1 C rate for 3 cycles) and after long-term cycling. (d) Equivalent circuit.

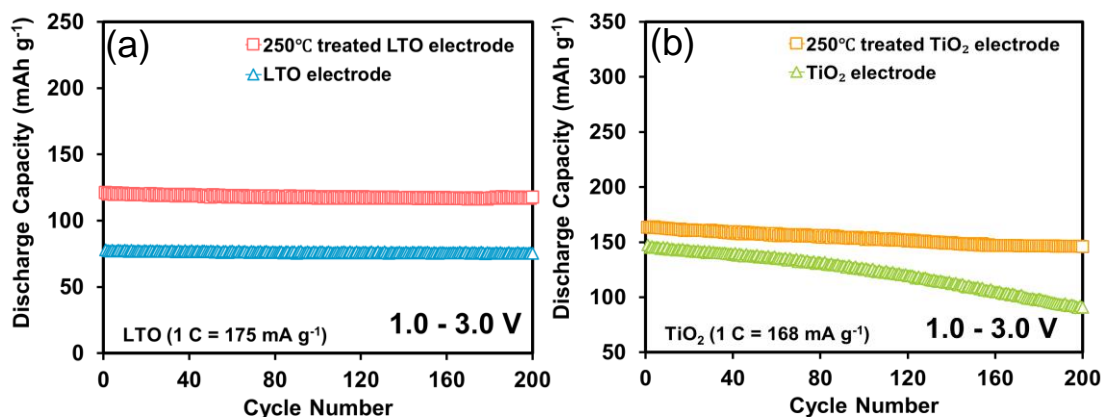


**Figure S8.** Cycling performance of (a) LTO and (b)  $\text{TiO}_2$  with and without  $250^\circ\text{C}$  treatment within a potential range of 1.0 – 3.0 V.

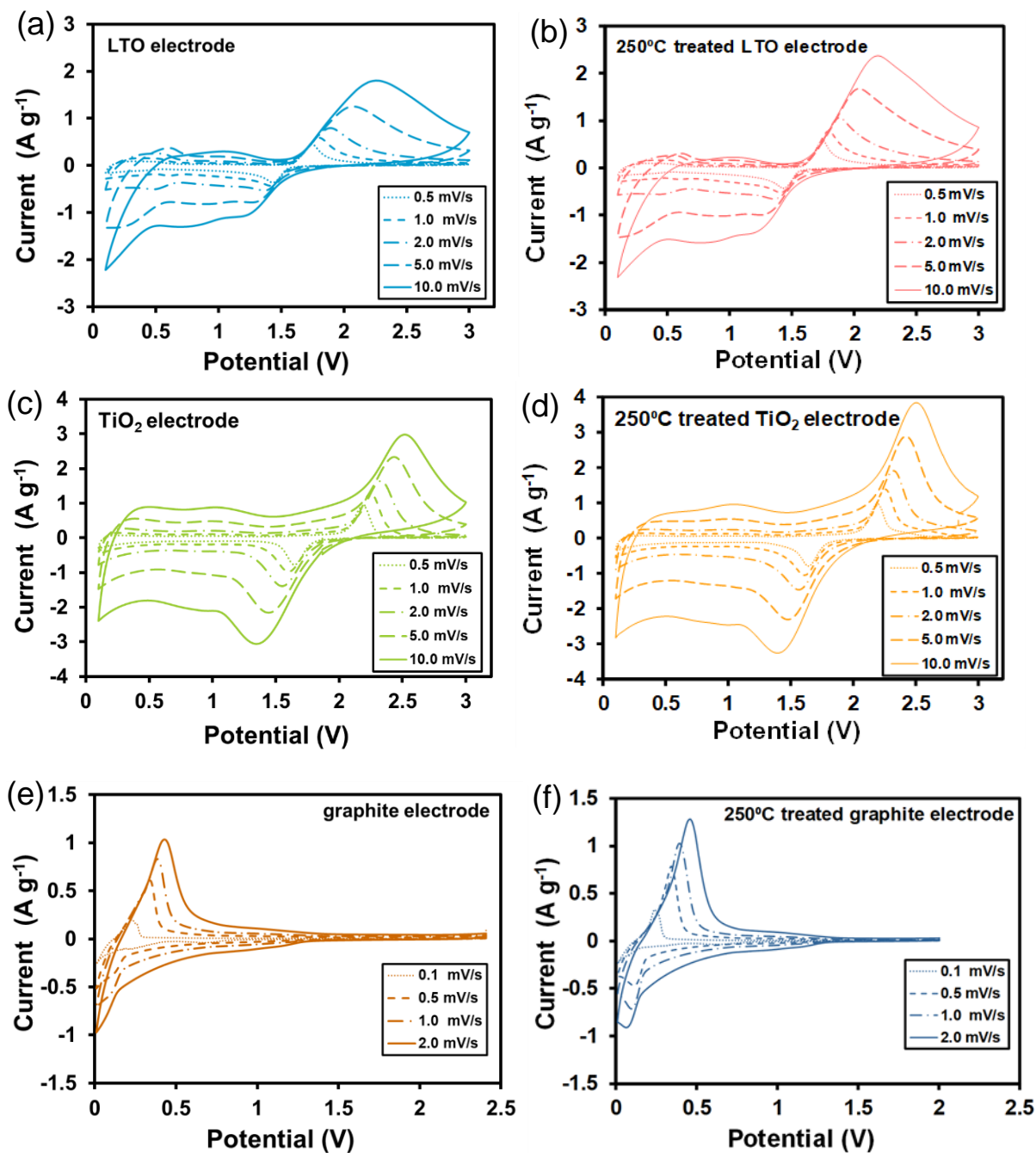


**Figure S9.** CV curves of (a) pristine LTO, (b) 250 °C treated LTO, (c) pristine  $\text{TiO}_2$ , and (d) 250 °C treated  $\text{TiO}_2$  electrodes at different scan rates of 0.5, 1.0, 2.0, 5.0, and 10.0  $\text{mV s}^{-1}$ . CV curves of (e) pristine graphite and (f) 250 °C treated graphite electrodes at different scan rates of 0.1, 0.5, 1.0, and 2.0  $\text{mV s}^{-1}$ .

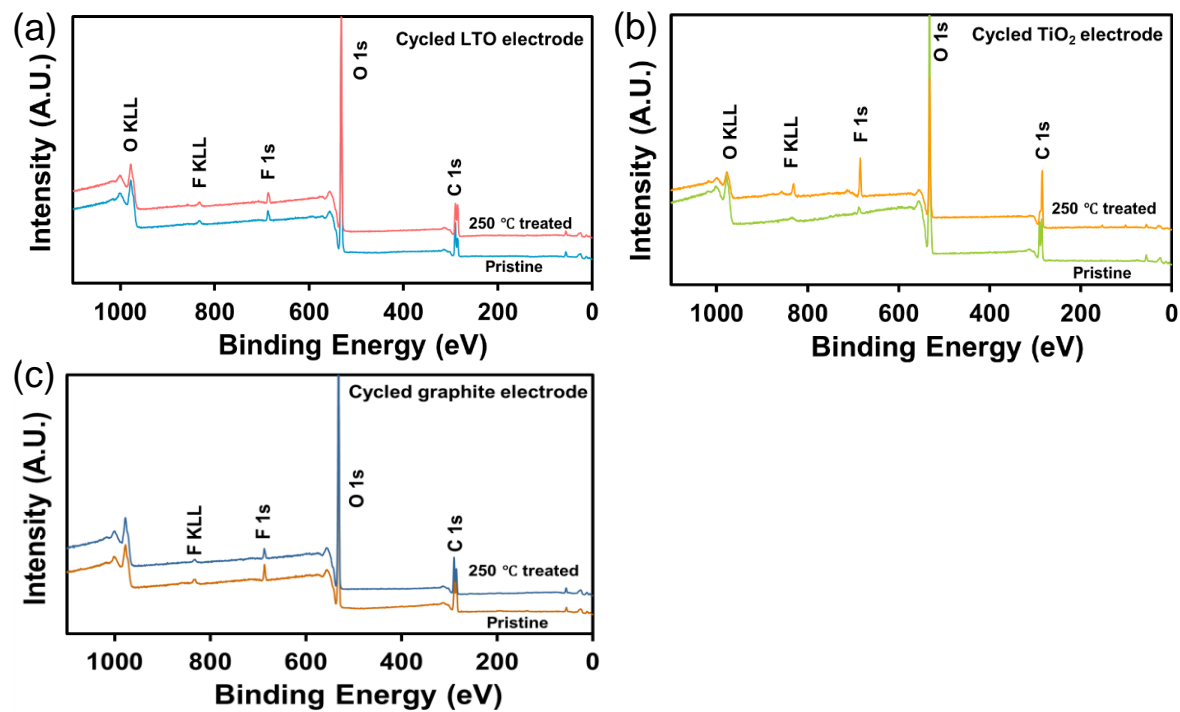


**Figure S10.** XPS survey spectra of electrodes: (a) LTO after 500 cycles of charge/discharge, (b)  $\text{TiO}_2$  after 1,000 cycles of charge/discharge, and (c) graphite after 500 cycles of charge/discharge.

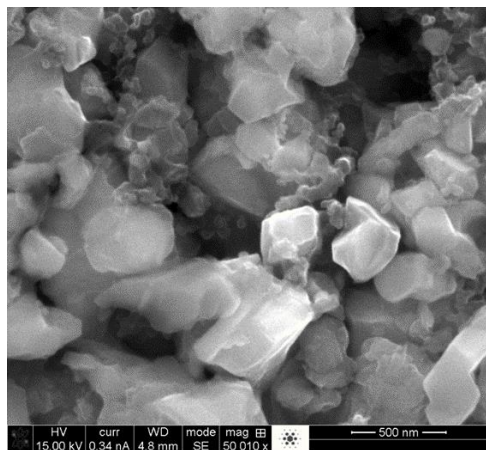


**Figure S11.** SEM image of fresh LTO electrode without 250 °C treatment.

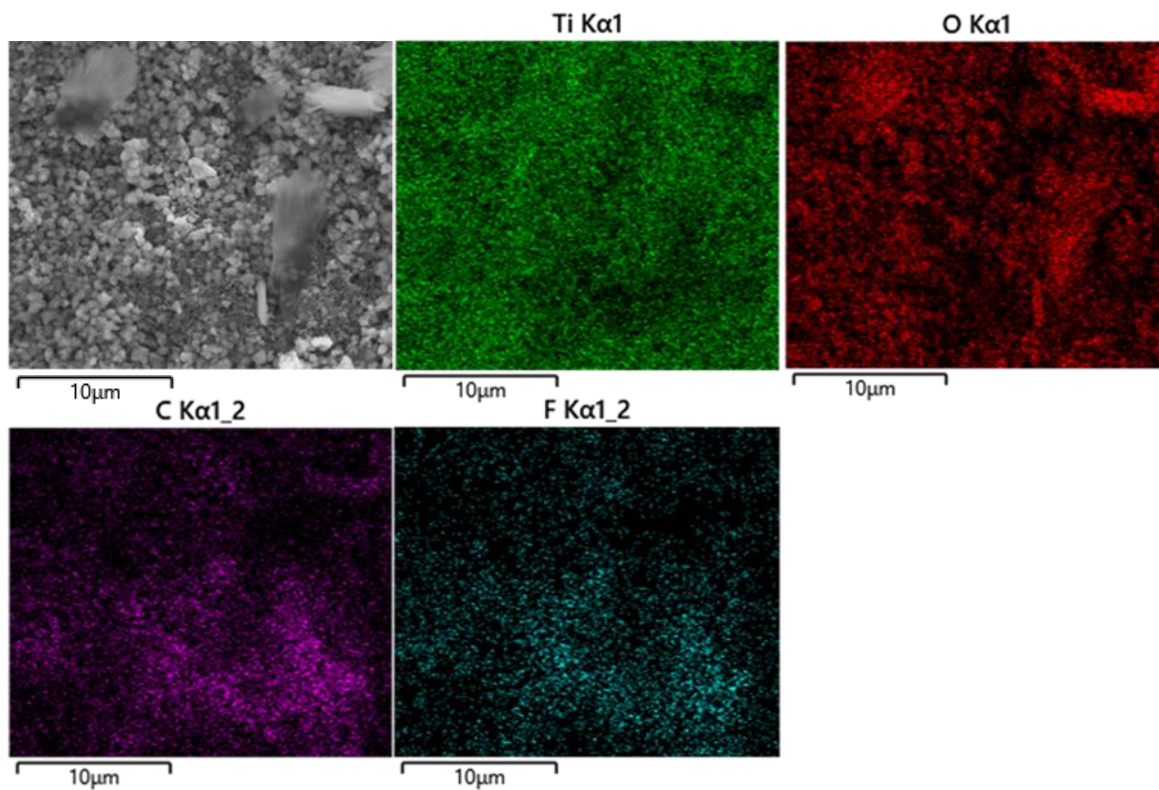


**Figure S12.** SEM image and EDS mapping of pristine LTO electrode after 500 cycles of charge/discharge.

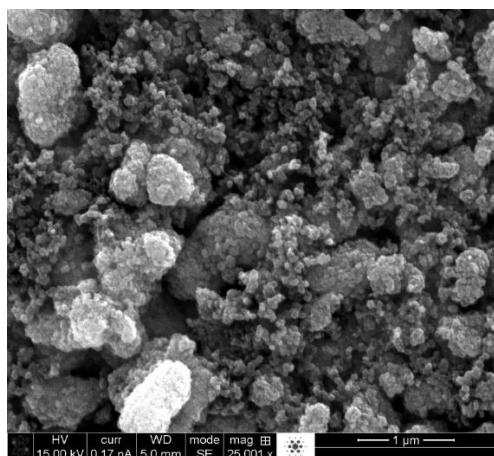


**Figure S13.** SEM image of fresh TiO<sub>2</sub> electrode with 250 °C treatment.



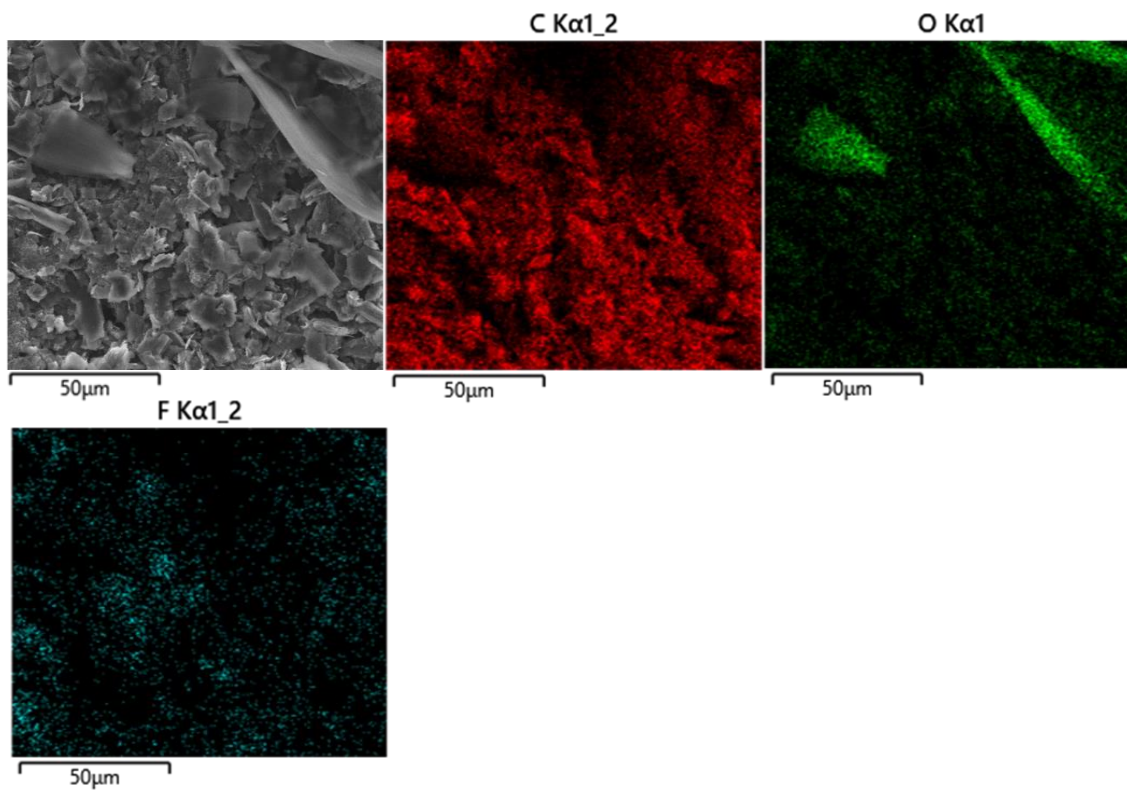


**Figure S14.** SEM image and EDS mapping of pristine graphite electrode after 500 cycles of charge/discharge.

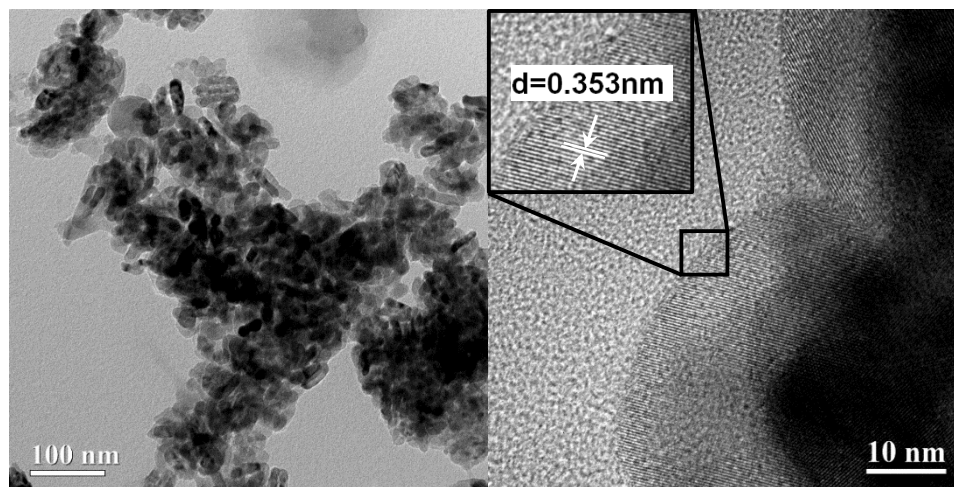


**Figure S15.** TEM images of pure  $\text{TiO}_2$  nanoparticles.